Power Coverage and Multipath Diversity for Indoor Distributed Antenna System Based on Wideband Channel Measurement at 6 GHz

Liang Xin†, Jianhua Zhang*, Fei Xiong, Yanliang Sun, Nan Sheng
Key Laboratory of Universal Wireless Communications, Ministry of Education
Wireless Technology Innovation Institute (WTI), Beijing University of Posts and Telecommunications
Beijing 100876, China
Email:†xinliang.jia@163.com, *jhzhang@bupt.edu.cn

***Abstract*—In this paper, power coverage characteristic and multipath diversity scheme for downlink simulcast distributed antenna system (DAS) are investigated based on a wideband channel measurement at 6 GHz for indoor scenario. With measured path loss (PL), power coverage property is analyzed. Compared with centralized antenna system (CAS), DAS can introduce 5-17 dB PL gain, and achieve a higher coverage ratio. Then, we propose a multipath diversity algorithm to improve the received power through introducing differential delay and phase rotation simultaneously at the transmitter (Tx). Based on the measured data, it has 1.67 dB power gain in line of sight (LOS) case averagely, better than the scheme without transmission control and multipath antenna diversity (MAD) algorithm.**

I. Introduction

Distributed antenna system (DAS), as a promising technology, has received quite a bit of interest [1-4]. As demonstrated in [2-4], it can reduce access distance to improve power coverage. However, the conclusions in [2] are based on assumed channel model, rather than real radio environment. Though experimental results for indoor DAS at 0.9 GHz, 1.9 GHz and 3.5 GHz are provided in [3, 4], few results are reported at 6 GHz or above, where abundant frequency resources can be exploited to meet the increasing demand for high data rates transmission. Moreover, since path loss (PL) exponent increases with carrier frequency [5], the propagation signals at 6 GHz would be easily attenuated with distance and obstruction, especially for indoor environment with rich scatters or obstacles. Thus to evaluate performance of DAS at 6 GHz for indoor scenario is imminent for future wireless communication.

In this work, we firstly evaluate power coverage characteristic of DAS in a simplified downlink simulcast scheme, where all the distributed antenna units (DAU) transmit completely the same signals, simultaneously. Based on measured channel at 6 GHz for indoor scenario, coverage advantage of DAS over centralized antenna system (CAS) is demonstrated.

However, the simplified simulcast scheme may bring about destructive summation of the signals from different DAUs, due to random phase of every radio link. In order to avoid it, multipath antenna diversity (MAD) algorithm in [6, 7] is proposed to allow some powerful multipath components (MCs) of different radio links to be separated in time, through intentionally leading differential delays into raw transmitted signals. So destructive combination of all the powerful MCs can be avoided to a great extent. Unfortunately, the MAD algorithm can not achieve the coherent superposition of powerful MCs, resulting in non-optimal performance. Thus, in this paper, a multipath diversity algorithm is proposed to make some powerful multipath components aligned in time and approximately co-phased (MPC), through transmission control. When phase angle of adjacent MCs changes mildly, it is possible to enable some powerful MCs sums constructively at Rx. Based on measured data, the superiority of the MPC algorithm has been verified in line of sight (LOS) and non-LOS (NLOS) case, respectively.

The rest of the paper is organized as follows. In Section II, the system model of DAS and fundamental principle are presented. Section III describes measurement equipment and environment. Power Coverage characteristics of DAS and performance of the MPC algorithm are analyzed in Section IV. Section V concludes the paper.

II. System Model and Fundamental Principle

We consider the following downlink simulcast DAS illustrated in Fig. 1, with L DAUs and single user equipment (UE) equipped with a receiving antenna. $x(t)$ denotes the raw signal at time t, which would be delayed by $\Delta\tau_i(t)$ and weighted by the phase rotation factor $e^{j\Delta\theta_i(t)}$ at the i^{th} branch. $h_i(t,\tau)$ indicates the time-variant wideband channel impulsive response (CIR) at the i^{th} radio link [7],

$$h_i(t,\tau) = \sum_{n=1}^{N_i(t)} \alpha_i(t,n) \cdot e^{j\theta_i(t,n)} \cdot \sigma(\tau - \tau_i(t,n)) \tag{1}$$

where $N_i(t)$ is the number of MCs. τ is the delay variable. $\tau_i(t,n)$, $\alpha_i(t,n)$ and $\theta_i(t,n)$ are discrete propagation delay, amplitude and phase angle of the n^{th} MC, separately. $\sigma(\cdot)$ is unit impulse function.

A. Power Coverage

For a simplified simulcast scheme, also referred as direct summation (DS) scheme without transmission control, where

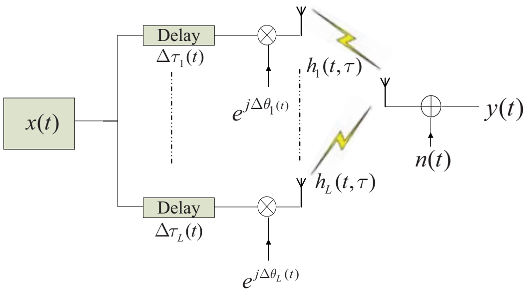

Fig. 1. The downlink simulcast scheme in DAS.

$\Delta\tau_i(t)$= 0 and $\Delta\theta_i(t)$= 0, for $i = 1, \ldots, L$ and any t, the received signal at UE is

$$y(t) = \sum_{i=1}^{L} h_i(t,\tau) * x(t) + n(t) = x(t) * \sum_{i=1}^{L} h_i(t,\tau) + n(t) \quad (2)$$

where the symbol $*$ indicates the operator of convolution, and $n(t)$ represents the additive thermal noise.

An equivalent CIR in DAS for the DS scheme, is introduced

$$\hat{h}(t,\tau) = \sum_{i=1}^{L} h_i(t,\tau) \quad (3)$$

In order to evaluate power coverage, PL is investigated, which is a measure of the average attenuation exerted by wireless channel. The PL of the i^{th} radio link and DAS can be calculated [4] by (4) and (5), respectively,

$$PL_i(d) = -10 \cdot \log_{10}\left(\mathrm{E}\left[\sum_{\tau} |h_i(t,\tau)|^2\right]\right) \quad (4)$$

$$PL_{\text{DAS}}(d) = -10 \cdot \log_{10}\left(\mathrm{E}\left[\sum_{\tau} \left|\hat{h}(t,\tau)\right|^2\right]\right) \quad (5)$$

where $\mathrm{E}[\cdot]$ denotes the average of many snapshots of CIR in the local area [4].

Then, log-distance (LGD) model [5] is used to model the PL for a single radio link,

$$PL(d) = A + n \cdot 10\log_{10}(d) + X_\sigma \quad (6)$$

where d is the distance between the transmitter (Tx) and the receiver (Rx). A denotes the PL intercept, and n is the PL exponent, representing the rate at which PL increases with distance. X_σ indicating the shadow fading, can be modeled as a zero-mean Gaussian random variable with standard deviation σ [5].

B. Multipath Diversity Algorithm

As L DAUs are separated spatially, propagation paths among different radio links may be independent or weakly correlated, which may bring about destructive summation in (2) to aggravate the received power, due to random phase. Therefore, $\Delta\tau_i(t)$ and $\Delta\theta_i(t)$ should be led into $x(t)$, and the received signal would be

$$\begin{aligned} \tilde{y}(t) &= \sum_{i=1}^{L} h_i(t,\tau) * \left(x(t - \Delta\tau_i(t)) \cdot e^{j\Delta\theta_i(t)}\right) + n(t) \\ &= \left(\sum_{i=1}^{L} h_i(t, \tau - \Delta\tau_i(t)) \cdot e^{j\Delta\theta_i(t)}\right) * x(t) + n(t) \end{aligned} \quad (7)$$

Similarly, an equivalent CIR $\tilde{h}(t,\tau)$ with transmission control is also introduced,

$$\tilde{h}(t,\tau) = \sum_{i=1}^{L} h_i(t, \tau - \Delta\tau_i(t)) \cdot e^{j\Delta\theta_i(t)} \quad (8)$$

In order to obtain a good received power, the parameters $\Delta\tau_i(t)$ and $\Delta\theta_i(t)$ should be calibrated according to the known channel information. Since for a specific $x(t)$, the received power depends on $\tilde{h}(t,\tau)$. Thus, we attempt to optimize the power of $\tilde{h}(t,\tau)$,

$$\begin{aligned} P &= \max_{\Delta\tau_i(t),\Delta\theta_i(t)} \left\{\sum_{\tau} \left|\tilde{h}(t,\tau)\right|^2 = \sum_{\tau} \left|\sum_{i=1}^{L} h_i(t, \tau - \Delta\tau_i(t)) \cdot e^{j\Delta\theta_i(t)}\right|^2\right\} \\ &\leq \max_{\Delta\tau_i(t)} \left\{\sum_{\tau} \left(\sum_{i=1}^{L} |h_i(t, \tau - \Delta\tau_i(t))|\right)^2\right\} \end{aligned} \quad (9)$$

The upper bound can hardly be achieved, for the basic condition is usually unattainable that all the MCs need to have the same phase at any t. Therefore, some algorithms with low complexity are presented for suboptimal diversity performance.

MAD Algorithm: In the MAD algorithm, only delay parameter $\Delta\tau_i(t)$ is introduced ($\Delta\theta_i(t)$ is zero). A powerful MCs window (MCW) is introduced for a CIR in any radio link, which includes some MCs adjacent to each other. A β dB threshold measured down from the peak path [6, 7] is used to determine the width of PMW. Then $\Delta\tau_i(t)$ is calculated according to the L determined PMWs, to make them well-separated in time. Therefore destructive superposition interference among all the propagation links is limited. However, the MAD algorithm can not exploit the potential diversity gain brought about by coherent superposition of propagation links, causing a non-optimal performance.

MPC Algorithm: In the MPC algorithm, delay and phase are introduced, simultaneously. Contrary to the MAD algorithm, differential delays are firstly introduced to make all the MCWs aligned in time. Then phase rotations are carried out to make them with close phases. The procedure of MPC algorithm is described as follows.

Procedure of MPC Algorithm:

- ***Step 1: Determine MCWs for*** L ***Links***
  We assume the number of components in the MCW as X. For the i^{th} $(i = 1, 2, \cdots, L)$ radio link, we use the $m_i(t)^{th}$ MC (obviously, $m_i(t) \leq N_i(t)$) to denote the peak path. If $m_i(t) \geq \lceil (X-1)/2 \rceil$, where $\lceil (X-1)/2 \rceil$ gives the smallest integer larger than $(X-1)/2$, X MCs adjacent to each other

which center on the peak path will be chosen. Otherwise, we chose the top X MCs, of which the MCW consists.

- ***Step 2: Introduce Delay***
  The L MCWs determined in step 1, may be not aligned in time, so delay should be introduced. Calibrate $\Delta\tau_i(t)$ according to the difference in time, to make all the MCWs aligned.
- ***Step 3: Rotate Phase Angle***
  When the MCWs have the same mean phase angles, they would be regarded to be in phase.
  The mean phase angle in a MCW is calculated by

$$\overline{\theta}= \sum_{k=1}^{X} \alpha_i{}^2(t, n_k) \times \theta_i(t, n_k) \tag{10}$$

  where the components in the MCW correspond with the $(n_1 - n_X)^{th}$ MCs. $\alpha_i{}^2(t, n_k)$ and $\theta_i(t, n_k)$ are power and phase angle of the n_k^{th} MC.
  Then, according to difference of mean phase angles, phase angle is rotated by $\Delta\theta_i(t)$ at the i^{th} branch to compensate the difference, so that all the MCWs have the same mean phase angle.

When phase variations within all the MCWs are small, constructive superposition of the MCWs can be achieved to lead to a better received power.

Metric: In order to evaluate performance for different diversity algorithms, power gain proposed in [7] is adopted as metric, which is the ratio (in dB) between combined power of L propagation links and summation of power in every individual propagation link,

$$G = 10 \cdot \log_{10}\left(\sum_{\tau} \left|\overline{h}(t,\tau)\right|^2 \Big/ \sum_{i=1}^{L} \sum_{\tau} |h(t,\tau)|^2 \right) \tag{11}$$

where $\overline{h}(t,\tau)$ is combined CIR of L links, it can be $\hat{h}(t,\tau)$ or $\tilde{h}(t,\tau)$.

III. Measurement Equipment and Environment

In order to evaluate power coverage and performance of the MPC algorithm in DAS, we conduct a channel measurement in Beijing University of Posts and Telecommunications (BUPT), China. The measured data are collected with Elektrobit Propsound channel sounder. Two stable rubidium frequency references are used for accurate synchronization between Tx and Rx. The measurement system parameters are detailed in Table I.

The campaign is conducted at the first floor inside a 7-floor building with the dimension of 120 m × 45 m × 6 m for each. The skeleton map of the first floor is shown in Fig. 2. The 4 DAUs with a single vertical-polarized dipole (VPD) for each, denoted as Tx1 ~ Tx4, transmit the same pseudo-random (PN) code sequences, and work in a time-division multiplexing (TDM) mode within a channel coherence time. The CIR is collected at Rx by a sliding correlator, which correlates the received signal with a synchronized copy of the transmitted PN sequence. Besides, Rx can move along routes denoted as route 1 ~ route 13 at the speed of 1-2 m/s during the measurement.

TABLE I
Measurement System Parameters

Parameter	Value
Center Frequency [GHz]	6
Bandwidth [MHz]	100
Transmitted Power [dBm]	24
DAU/Rx Antenna Height [m]	2.7/2
DAU/Rx Elements	4/1
PN Code Length [chips]	255
Delay Resolution [ns]	10

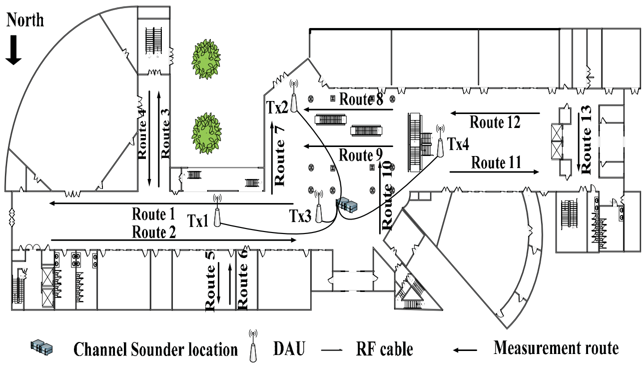

Fig. 2. The skeleton map of measurement scenario in BUPT for indoor DAS.

IV. Results and Analysis

A. Power Coverage for DAS

In DAS discussed in this part, 4 DAUs are all employed. If only one DAU is utilized, it degenerates into a single link system (or CAS). The PLs for CAS and DAS are calculated by (4) and (5), respectively, on all the measured routes shown in Fig. 2. To make sure the fairness in performance comparison, the total transmitted power in DAS and CAS is the same, which is controlled in data processing. In Fig. 3, DAS has better performance than CAS, and it has 5.1 dB, 8.4 dB, 5.9 dB and 17.2 dB PL gain over 4 cases (Tx1 ~ Tx4) in CAS, respectively.

Besides, coverage ratio is introduced to quantify coverage performance. The coverage ratio is confined by PL threshold assumed as $PL_{\text{threshold}}$, when the transmitted power is fixed,

$$P_{\text{ratio}} = \frac{\sum_{k=1}^{K} P_{r,k}}{K} \tag{12}$$

where

$$P_{r,k} = \begin{cases} 1; & PL^k \le PL_{\text{threshold}} \\ 0; & PL^k > PL_{\text{threshold}} \end{cases} \tag{13}$$

where K is the number of measured results on all the routes. PL^k is the PL in CAS or DAS of the k^{th} measured result.

Through assuming the coverage ratio in DAS, $PL_{\text{threshold}}$ can be obtained. Then substitute the $PL_{\text{threshold}}$ and PLs in

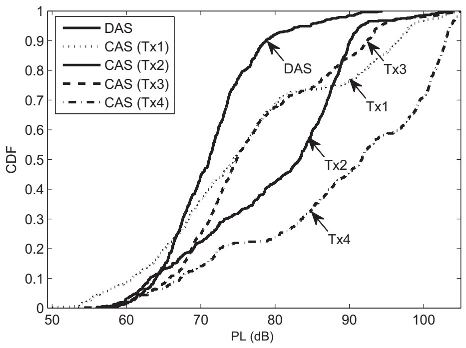

Fig. 3. CDFs of PLs for DAS and CAS.

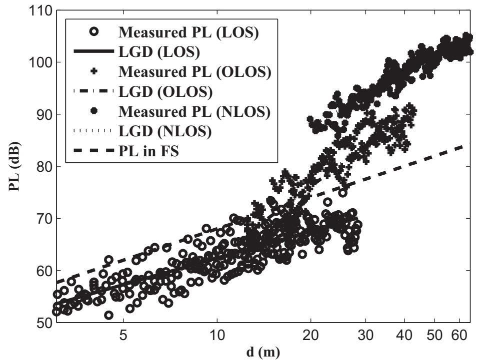

Fig. 4. PLs for indoor scenario at 6 GHz.

CAS into (12) and (13) again, coverage ratio in CAS will be determined. The coverage ratios in DAS and CAS are summarized in Table II, from which DAS has the highest coverage ratio.

TABLE II
Coverage Ratios in DAS and CAS

Antenna Configuration	Coverage Ratio			
DAS	70%	80%	90%	100%
CAS (Tx1)	47%	55%	66%	85%
CAS (Tx2)	30%	33%	40%	97%
CAS (Tx3)	43%	55%	65%	95%
CAS (Tx4)	21%	22%	23%	58%

In all, compared with CAS, DAS has better power coverage characteristic. To further analyze the reason, large scale fading is investigated by modeling the PL for every radio link.

For a certain DAU, 13 routes are measured: some routes are LOS routes; some are obstructed LOS (OLOS) due to partially obstruction by pillars or walls; the others are NLOS routes where the received signal is obstructed completely by walls. The 4 DAUs can introduce 52 equivalent routes, equivalently. Then PLs are modeled, respectively, according to the propagation condition with LGD model.

TABLE III
PL models for indoor scenario at 6 GHz

Case	PL Models [in dB]
LOS	$PL(d) = 45.4 + 17.0 \cdot \log_{10}(d) + X_\sigma, \sigma = 2.7$
OLOS	$PL(d) = 18.1 + 44.6 \cdot \log_{10}(d) + X_\sigma, \sigma = 3.1$
NLOS	$PL(d) = 44.6 + 33.1 \cdot \log_{10}(d) + X_\sigma, \sigma = 1.5$

As shown in Fig. 4, the PLs at 6 GHz in LOS case are better than free space propagation scenario (FS), where the receive signal has only LOS path, without reflected and scattered components. It is reasonable that in an enclosed indoor scenario, received signals are the summation of many multipath components. In addition to LOS component, other components reflected by floors, walls or other objects, can be powerful enough. The similar results are observed at 2.4 GHz, 4.75 GHz and 11.5 GHz [5]. In OLOS case, the propagation signals are partially obstructed. Thus, at some locations, the PLs are better than FS where LOS propagation is dominating. While in other cases, the signals may experience more attenuation than FS due to obstruction by walls or pillars. Finally for NLOS case, received signals are greatly attenuated. The PLs in NLOS case are the worst. At $d = 20$ m, PL in NLOS case is 20 dB worse than that in LOS case, 13.1 dB worse when compared with OLOS case.

Besides, the exponent in LOS case is smaller than those in OLOS and NLOS case, thus PL in LOS case would change milder with distance. Since the transmit antennas in DAS are in different locations, thus UE can access to the nearest DAU. The reduced distance can avoid obstruction and make sure more LOS probability, which can lead to less attenuation by distance and obstruction. Therefore, DAS can have better received signal strength and possess a good coverage ratio.

B. Multipath Diversity for DAS

The measured data from Tx1, Tx2 and Tx3 ($L = 3$) are used to evaluate the performance of MPC algorithm. When all the radio links are LOS propagation (e.g. Rx on route 9 and 10 etc.), it is considered as the LOS case of DAS. While for NLOS case of DAS, it should make sure all the radio links are NLOS propagation (e.g. Rx on route 5, 6 and 14 etc.).

Since phase angle dispersion may influence constructive summation of MCWs, which impacts on the performance of the MPC algorithm, the phase angle dispersion should be investigated before evaluation of the MPC algorithm. The root mean square (RMS) phase angle spread is introduced to measure phase angle dispersion in the MCW, which is the second central moment of the phase angle power profile.

TABLE IV
Average RMS Phase Angle Spread (in Degree) in LOS and NLOS case

Case	Tx1	Tx2	Tx3
LOS	48.1°	51.5°	45.5°
NLOS	49.9°	47.0°	48.1°

From Table IV, the average RMS phase angle spreads in the MPW (here $X = 5$) for all the links are smaller than 60

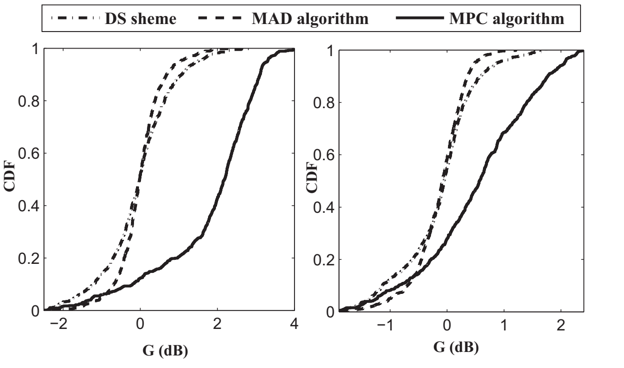

Fig. 5. Performance comparison in LOS and NLOS case (β = 6 dB in the MAD algorithm, and X = 5 in the MPC algorithm).

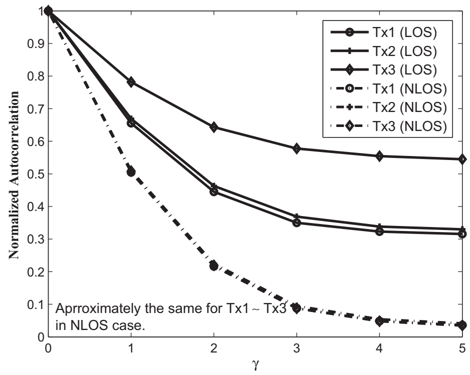

Fig. 6. Average phase angle autocorrelation for LOS and NLOS case.

degrees in both LOS and NLOS cases. Thus it is possible to make some MCs sum coherent with phase angle rotation.

In Fig. 5, the MPC algorithm can achieve the maximum power gain averagely in both LOS and NLOS cases. For LOS case, it has 1.79 dB more power gain than the DS scheme averagely. But for the MAD algorithm, it is only 0.1 dB power gain in average over the DS scheme.

Besides, from Table IV, the average RMS phase angle spreads in LOS and NLOS cases are close. However, in LOS case, MPC algorithm can introduce 1.67 dB power gain in average, and has only 0.42 dB power gain in NLOS case. In order to find out the reasons resulting in the difference between two scenarios, phase angle autocorrelation characteristic is introduced, which is defined for a single propagation link,

$$f_i(\gamma) = \sum_{n=1}^{N_i(t)} \theta_i(t,n) \cdot \tilde{\theta}_i(t, n+\gamma); \gamma = 0, 1, 2, \ldots, X. \quad (14)$$

where

$$\tilde{\theta}_i(t, n+\gamma) = \begin{cases} \theta_i\left(t, n+\gamma - N_i(t)\right); n+\gamma > N_i(t) \\ \theta_i(t, n+\gamma) \quad ; n+\gamma \leq N_i(t) \end{cases} \quad (15)$$

As shown in Fig. 6, LOS case has comparatively strong average phase angle autocorrelation. The MPC algorithm would have better performance. It is reasonable that for LOS case, its components in the MCW would be highly correlated in phase angle. If RMS phase angle spread is not large, all the components in the MCW are apt to constructive summation, simultaneously, to lead to a good power gain. Thus, the MPC algorithm is more suitable to the scenario with highly correlated phase angle.

Further more, in the MPC algorithm, parameter X is a variable. Generally, the small value of parameter X would achieve good diversity performance. Considering the influence of phase angle dispersion, guidelines are presented in [8] to determine the parameter X. Besides, the robustness of the MPC algorithm is also evaluated in [8] with the imperfect introduction of delays and phase rotation etc.

V. Conclusions

In this paper, coverage property and multipath transmit algorithm for DAS are studied based on wideband channel measurement. As regards the power coverage, DAS can yield 5-17 dB PL gain to contribute to a better coverage ratio. Beside, the proposed MPC algorithm can improve the received power, and performs better than the DS scheme and the MAD algorithm for both LOS and NLOS cases, which also would be affected by the phase angle autocorrelation characteristic and phase angle dispersion.

Acknowledgments

This research is supported by China Information Technology Designing & Consulting Institute Ltd (CITC)-School of Information and Communication Engineering (SICE) in BUPT Graduate Innovation Fund for 2011, and the National Natural Science Foundation of China under Grant 61171105.

References

[1] S. Zhou, M. Zhao, X. Xu, J. Wang, and Y. Yao, "Distributed wireless communication system: a new architecture for future public wireless access," *IEEE Wireless Communication Magazine*, March 2003.

[2] D. Castanheira and A. Gameiro, "Distributed antenna system capacity scaling [coordinated and distributed mimo]," *IEEE Wireless Communication Magazine*, vol. 17, no. 3, pp. 68-75, 2010.

[3] A. Arredondo, D. Cutrer, J. Georges, and K. Lau, "Techniques forimproving in-building radio coverage using fiber-fed distributed antenna networks," *in Proceedings of IEEE Vehicular Technology Conference (VTC 1996)*, pp. 1540-1543, 1996.

[4] X. Hu, Y. Zhang, Y. Jia, S. Zhou, and L. Xiao, "Power coverage and fading characteristics of indoor distributed antenna systems," *Proceedings of Fourth International Conference on Communications and Networking in China (Chinacom 2009)*, pp.1-4, 2009.

[5] G. Janssen, P. Stigter and R. Prasad, "Wideband indoor channel measurements and BER analysis of frequency selective multipath channels at 2.4 GHz, 4.75 GHz and 11.5 GHz," *IEEE Transactions on vehicular technology*, vol. 44, no. 10, pp. 1272-1288, 1996.

[6] F. Tong, I. Glover, S. Pennock, P. Shepherd, and N. Davies, "Indoor distributed antenna experiments," *in Proceedings of 14th IST Mobile and Wireless Communications Summit*, 2005.

[7] H. Hu, Y. Zhang, and J. Luo, *Distributed antenna systems: open architecture for futureWireless communications*, Auerbach Publication, 2007.

[8] L. Xin, J. Zhang, J. Gao, and X. Li, "Transmit diversity in simulcast system based on wideband channel measurement at 6 GHz," unpublished.